Dentistry 3000

Vol 14, No 2 (2026)
ISSN 2167-8677 (online)
DOI 10.5195/d3000/2026.1492

Molecular Mechanisms of Sulforaphane-Mediated Biofilm and Virulence Regulation of *Streptococcus mutans*

Tabark Ammar, Mohameed Flyyiah Traef, Susan Zwyea
Middle Technical University, College of Health and Medical Techniques, Baghdad, Iraq

Abstract

Dental caries is the most prevalent biofilm-mediated disease worldwide, and *Streptococcus mutans* is its principal etiological agent. Because broad-spectrum antiseptics disturb the commensal flora and may drive resistance, anti-virulence strategies based on safe natural products are increasingly sought. Sulforaphane (SFN), a cruciferous isothiocyanate, has documented bacteriostatic activity, but its effect on clinical *S. mutans* isolates and on the molecular determinants of cariogenicity is poorly defined. Twenty-five clinical *S. mutans* isolates from carious lesions and dental plaque were challenged with SFN (Sigma-Aldrich) in 0.5% DMSO. Antibacterial activity was assessed by agar-well diffusion and broth microdilution (MIC/MBC) with chlorhexidine as positive control and triphenyltetrazolium chloride as viability indicator. Biofilm formation and the anti-biofilm effect were quantified by the crystal-violet microtiter assay. Expression of *gtfC* (EPS synthesis), *ldh* (acidogenicity) and *sodA* (oxidative-stress defense) was measured by qRT-PCR at sub-MIC (625 µg/mL) using *16S rRNA* as reference gene ($2^{-\Delta\Delta Ct}$ method). SFN showed dose-dependent activity (zone of inhibition 17.8 ± 0.55 mm at 5%). The MIC was 1250 µg/mL for all isolates; no killing occurred up to 2500 µg/mL (MBC > 2500 µg/mL; MBC/MIC > 2), indicating a bacteriostatic, anti-virulence action. Eighteen isolates were strong, 3 moderate and 4 weak biofilm producers; SFN suppressed biofilm formation dose-dependently ($p < 0.0001$). At sub-MIC, SFN down-regulated *gtfC* by ≈99.5% (≈195-fold), *sodA* by ≈97.2% (≈35-fold) and *ldh* by ≈97.0% (≈34-fold) (all $p < 0.01$). *gtfC*/*sodA* expression was strongly correlated ($r = 0.72$), and PCA cleanly separated treated from untreated profiles (PC1 = 70.8%). SFN is a bacteriostatic, multi-target anti-virulence agent against clinical *S. mutans*, simultaneously disabling biofilm scaffolding, acidogenesis and oxidative-stress defense without killing the cell — a profile favorable for caries control with low resistance-selection pressure.

Open Access

Citation: Ammar T et al. (2026) Molecular Mechanisms of Sulforaphane-Mediated Biofilm and Virulence Regulation of *Streptococcus mutans*. Dentistry 3000. 1:a001 doi:10.5195/d3000.2026.1492
Received: July 2, 2026
Accepted: July 5, 2026
Published: August 14, 2026

Email: Tabark.ammar.2t@gmail.com

Introduction

Dental caries remains one of the most widespread chronic non-communicable diseases of humans, affecting billions of individuals across all age groups and imposing a substantial global health and economic burden [1,2]. The disease is now understood not as a simple infection but as a diet-driven, biofilm-mediated ecological shift, in which frequent exposure to fermentable carbohydrates selects for acidogenic and aciduric organisms that progressively demineralize the dental hard tissues [2,3].

Within the complex oral microbiota, *Streptococcus mutans* is regarded as the principal etiological agent of caries [1,4]. Its cariogenic potential rests on a coordinated triad of virulence properties. First, sucrose-dependent adhesion and the synthesis of extracellular polysaccharides (EPS) allow the organism to colonize the tooth surface and build a cohesive, diffusion-limiting biofilm matrix [3,5,6]. Second, prolific fermentation of dietary sugars to organic acids (acidogenicity) lowers plaque pH below the critical threshold for enamel dissolution [7,8]. Third, the capacity to grow and metabolize under acidic and oxidatively challenging conditions (aciduricity and

Vol 14, No 2 (2026) DOI 10.5195/d3000/2026.1492

aerotolerance) enables *S. mutans* to outcompete less tolerant commensals and to perpetuate the cariogenic state [7,9].

These properties are governed by defined molecular effectors. The glucosyltransferases, especially the products of *gtfB* and *gtfC*, polymerize sucrose into water-insoluble glucans that form the adhesive scaffold of dental plaque and are widely regarded as the single most important virulence determinant of cariogenic biofilm [5,6,10]. Lactate dehydrogenase, encoded by *ldh*, catalyzes the terminal reduction of pyruvate to lactic acid and is the dominant route of acid end-product formation [8,11]. Survival under the resulting oxidative and acid stress depends in part on detoxifying enzymes such as superoxide dismutase (*sodA*), which dismutates superoxide radicals and protects the cell during the aerobic and redox fluctuations of the plaque environment [9,12].

Conventional chemical control relies heavily on broad-spectrum antiseptics such as chlorhexidine. Although effective, these agents act indiscriminately against commensal and pathogenic species alike, may cause local side effects, and contribute to the broader problem of antimicrobial resistance [13]. This has stimulated interest in an alternative paradigm: anti-virulence therapy, in which the pathogenic behavior of an organism is disarmed without necessarily killing it, thereby preserving the protective commensal community and minimizing the selective pressure that drives resistance [13-15].

Sulforaphane [SFN; 1-isothiocyanato-4-(methylsulfinyl)butane] is an aliphatic isothiocyanate derived from the glucosinolate glucoraphanin, which is especially abundant in broccoli and other cruciferous vegetables [16,17]. Its defining structural feature is a highly electrophilic –N=C=S group that reacts readily with cellular nucleophiles, particularly protein thiols, allowing it to modulate multiple enzymatic and regulatory targets simultaneously [16,18]. SFN has been extensively characterized for cytoprotective, Nrf2-modulating, anti-inflammatory and anticancer activities, and displays an excellent safety profile in numerous preclinical and clinical studies [19,20]. In the antimicrobial sphere, SFN exerts bacteriostatic effects against a range of pathogens through diverse mechanisms encompassing biofilm interference, enzyme inhibition, energy-metabolism disruption and stress-response modulation [18,21-23].

Despite this promise, evidence for SFN activity against *S. mutans* remains limited. A recent study demonstrated inhibition of the laboratory reference strain UA159 and caries control in a rat model, primarily through suppression of glucosyltransferase and acid-production genes and the quorum-sensing *comCDE* system [24]. However, two important gaps persist: the activity of SFN against genetically diverse clinical isolates has not been characterized, and its impact on the oxidative-stress defense axis (*sodA*) has not been examined. Addressing these gaps is essential for judging the translational potential of SFN.

The present study therefore had two aims: (i) to determine the antibacterial and anti-biofilm activity of SFN against 25 clinical *S. mutans* isolates recovered from carious lesions and dental plaque; and (ii) to define the molecular basis of SFN-mediated virulence regulation by quantifying its effect on three complementary virulence axes — EPS synthesis (*gtfC*), acidogenicity (*ldh*) and oxidative-stress defense (*sodA*). We hypothesized that SFN attenuates *S. mutans* cariogenicity through a sub-lethal, multitarget mechanism rather than through bacterial killing.

Material and Methods

A cross-sectional study was conducted on 35

Bacterial isolates and culture conditions

Carious lesions and dental plaque were selected as the sampling source because dental caries is the clinical outcome of a pathogenic *S. mutans* biofilm rather than a separate entity: the organism initiates caries only after adhering to the tooth surface and forming a mature biofilm. Isolates recovered from active carious sites therefore represent clinically validated, strongly biofilm-forming strains that have already demonstrated cariogenic potential in vivo, making them a more relevant model for studying biofilm formation and its inhibition than laboratory reference strains.

Twenty-five (n = 25) clinical isolates of *S. mutans* were recovered from carious lesions and supragingival dental plaque. Presumptive identification was based on growth and characteristic colony morphology on Mitis-Salivarius-Bacitracin (MSB) agar. Species identity was subsequently confirmed by the automated VITEK system (biochemical identification) and further verified at the molecular level by detection of the *16S rRNA* gene, ensuring accurate identification of all isolates prior to testing. Confirmed isolates were maintained on blood agar and incubated anaerobically under 5% CO_2 (candle-jar system) at 37 °C for 48 h. For experimental work, isolates were sub-cultured in Tryptic Soy Broth (TSB) without glucose for susceptibility testing, and in TSB supplemented with glucose for biofilm and molecular assays, and grown to the logarithmic phase. Inocula were standardized to a 0.5 McFarland turbidity (1.5×10^8 CFU/mL) at OD_{600}, then diluted to the required working density (1×10^6 CFU/mL for MIC).

Preparation of sulforaphane and control solutions

A 0.5% DMSO solution was prepared as the solvent vehicle. Sulforaphane (Sigma-Aldrich, USA) was dissolved in 0.5% DMSO to yield a 10% (100 mg/mL) stock, homogenized by magnetic stirring for 30 min and stored at −20 °C. Working concentrations were obtained by serial dilution in 0.5% DMSO. Chlorhexidine (CHX) served as the positive antibacterial control, 0.5% DMSO as the solvent control, and sterile broth as the negative (sterility) control. Bacterial viability in the MIC assay was visualized using 2,3,5-triphenyltetrazolium chloride (TTC, 5 mg/mL), which is reduced by metabolically active cells to red, water-insoluble formazan [25].

Agar-well diffusion assay

Preliminary antibacterial screening was performed by agar-well diffusion on Mueller-Hinton agar. Lawns of each standardized isolate were prepared, and 5-mm wells were charged with 100 µL of SFN at 5% (50 mg/mL), 2.5% (25 mg/mL), 1.25% (12.5 mg/mL) or 0.62% (6.2 mg/mL). After anaerobic incubation (5% CO_2, 37 °C, 24 h), inhibition-zone diameters were measured in millimeters and recorded as mean ± SD across the 25 isolates.

Minimum inhibitory and bactericidal concentrations (MIC/MBC)

MIC was determined by broth microdilution in 96-well microtiter plates. Two-fold serial dilutions of SFN spanning 2500, 1250, 625, 313, 156, 78, 39 and 19.5 µg/mL were prepared in TSB and inoculated with 1 × 106 CFU/mL. CHX (serial dilutions from 128 µg/mL) was the positive control, 0.5% DMSO the solvent control and uninoculated broth the negative control. After incubation (37 °C, 24 h, 5% CO2), 20 µL of TTC (5 mg/mL) was added and plates were re-incubated in the dark; colorless wells indicated growth inhibition and red/pink wells indicated viable growth. Absorbance was read at 490 nm and the percentage of inhibition computed against controls. The MIC was the lowest concentration preventing visible growth.

The MBC of SFN was evaluated by sub-culturing the colorless (growth-inhibited) wells of the MIC plates at the four highest concentrations (2500, 1250, 625 and 313 µg/mL). A loopful (10 µL) from each clear well of all 25 isolates was streaked onto blood agar and incubated anaerobically under 5% CO2 at 37 °C for 48 h. After incubation, plates were examined for visible bacterial colony growth. The MBC was defined as the lowest concentration producing no colony growth, and the MBC/MIC ratio was used to classify the agent as bactericidal (≤ 2) or bacteriostatic (> 2).

Biofilm formation assay

Biofilm-forming capacity was quantified by the crystal-violet microtiter-plate method [34,35]. Standardized isolates were cultured in TSB

Vol 14, No 2 (2026) DOI 10.5195/d3000/2026.1492

with 1% glucose in 96-well U-bottom plates (in triplicate; 37 °C, 48 h, 5% CO_2). Planktonic cells were removed by triple PBS washing; adherent biofilm was fixed with absolute methanol, stained with 0.1% crystal violet, washed, and solubilized with 33% glacial acetic acid. Absorbance was read at 600 nm. Using the cut-off optical density (OD_c), isolates were graded as non-biofilm, weak, moderate or strong producers [26].

Anti-biofilm assay

The inhibitory effect of SFN on biofilm development was assessed in duplicate against five concentrations (1250, 625, 313, 156 and 78 µg/mL). SFN and standardized inoculum were co-incubated in TSB with 1% glucose (37 °C, 48 h, 5% CO_2); biofilms were then processed and quantified as in Section 2.5. Biofilm inhibition was expressed relative to the untreated biofilm control, and dose-response significance was evaluated statistically.

RNA extraction and quantitative RT-PCR

For transcriptional analysis, each isolate was prepared in parallel as an untreated control and an SFN-treated culture at sub-MIC (625 µg/mL), so that observed changes reflected genuine virulence modulation rather than loss of viability. Biofilm cells were lysed in TRIzol and total RNA was extracted following the manufacturer protocol (chloroform phase separation, isopropanol precipitation, 70% ethanol washing, rehydration in nuclease-free water). RNA was reverse-transcribed to cDNA, and target transcripts were amplified by SYBR-Green real-time PCR (CFX96, Bio-Rad). Expression of *gtfC*, *ldh* and *sodA* was normalized to the housekeeping gene *16S rRNA*, and relative expression (fold change) was computed by the comparative $2^{-\Delta\Delta Ct}$ method [27]. Gene-specific primers are listed in Table 1.

Statistical analysis

Data are presented as mean ± standard deviation. Because gene-expression fold-change values were non-normally distributed and contained outliers, between-group differences (control vs SFN) were tested with the non-parametric Mann-Whitney U test; dose-response biofilm data were analyzed by analysis of variance. A p-value < 0.05 was considered significant. Pearson correlation and principal component analysis (PCA) were used to explore co-expression structure among the three genes.

Ethics statement

The study was reviewed and approved by the Medical Ethics Committee of Middle Technical University, Baghdad, Iraq (Reference No. MEC: 121; approval date 07/05/2025), and conducted in accordance with the Declaration of Helsinki and ICH-GCP guidelines.

Results

Antibacterial activity by agar-well diffusion

SFN displayed clear, concentration-dependent antibacterial activity against all 25 clinical isolates. The mean inhibition-zone diameter rose progressively with concentration, from 10.9 ± 1.54 mm at 0.62% to 13.7 ± 0.74 mm at 1.25%, 14.8 ± 0.58 mm at 2.5% and 17.8 ± 0.55 mm at 5% (Table 2, Figure 1). The narrow standard deviations at higher concentrations indicate a consistent response across the genetically diverse isolate collection.

Minimum inhibitory and bactericidal concentrations

In broth microdilution, the MIC of SFN was uniform across the collection at 1250 µg/mL (1.25%). The mean percentage of inhibition declined steeply with dilution: 91.8% at 2500 µg/mL and 90.2% at the MIC (1250 µg/mL), falling to 44.0% at 625 µg/mL, 33.5% at 313 µg/mL and progressively to 2.3% at 19.5 µg/mL (Table 3, Figure 2). When the colorless (growth-inhibited) wells at 2500, 1250, 625 and 313 µg/mL were sub-cultured onto blood agar, visible colony growth appeared for all 25 isolates at every concentration tested; no bactericidal endpoint was therefore reached within the examined range (MBC > 2500 µg/mL). The resulting MBC/MIC ratio (> 2) classifies SFN as a bacteriostatic agent against clinical *S. mutans*, consistent with an anti-virulence rather than a microbicidal mode of action.

Biofilm-forming capacity of the isolates

All 25 isolates were confirmed biofilm producers, but with differing intensity. The majority — 18 isolates (72%) — were strong producers, while 3 (12%) were moderate and 4 (16%) were weak (Table 4, Figure 3). This predominance of strong biofilm formers underscores the cariogenic relevance of the collection and provides a stringent test bed for anti-biofilm intervention.

Anti-biofilm activity of SFN

SFN inhibited biofilm formation in a clearly dose-dependent manner across the tested range (78–1250 µg/mL). The mean biofilm optical density (OD_{600}) of the untreated biofilm control was 0.96, and decreased progressively with increasing SFN concentration to 0.72 at 78 µg/mL, 0.63 at 156 µg/mL, 0.56 at 313 µg/mL, 0.49 at 625 µg/mL and 0.41 at 1250 µg/mL (Figure 4). The reductions at 313, 625 and 1250 µg/mL were highly significant versus the untreated control ($p < 0.0001$), and the effect at 156 µg/mL was also significant ($p < 0.01$). The isolate-level heatmap confirms that this suppression was consistent across the collection, with the strongest decrease at and approaching the MIC. The parallel between the anti-biofilm dose-response and the growth-inhibition profile indicates that SFN curtails biofilm development at concentrations at and below those required to limit planktonic growth.

SFN down-regulates virulence-associated genes

Changes in gene expression can provide important information regarding responses to different treatments [40]. At sub-MIC (625 µg/mL), SFN profoundly suppressed all three target genes relative to untreated controls (Table 5, Figures 5–6). Expression of *gtfC* decreased from 2.571 to 0.013, a reduction of approximately 99.5% (≈195-fold) and the largest effect observed (Mann-Whitney $p = 1.2 \times 10^{-6}$). *sodA* fell from 1.732 to 0.049 (≈97.2%, ≈35-fold; $p = 3.6 \times 10^{-4}$), and *ldh* from 2.787 to 0.082 (≈97.0%, ≈34-fold; $p = 7.4 \times 10^{-3}$). The uniformity of these reductions across the three functional axes is evident in the expression heatmap (Figure 5) and in the sample-level distributions, which show a consistent downward shift after treatment (Figure 6).

Coordinated, multi-gene response

The three genes responded in a coordinated rather than independent manner. Pearson analysis revealed a strong positive correlation between *gtfC* and *sodA* (r = 0.72) and a moderate correlation between *sodA* and *ldh* (r = 0.58), with a weaker link between *gtfC* and *ldh* (r = 0.36) (Figure 7). Principal component analysis separated treated from untreated isolates along the first principal component, which alone explained 70.8% of the total variance (PC2 = 21.7%) (Figure 8). Together these analyses indicate that SFN imposes a distinct, integrated multi-gene expression signature, consistent with a multi-target mechanism affecting adhesion, acidogenesis and oxidative defense simultaneously.

Discussion

This study provides the first integrated characterization of sulforaphane activity against clinical *S. mutans* isolates, linking phenotypic antibacterial and anti-biofilm effects to the transcriptional regulation of three complementary virulence axes. The central finding is that SFN attenuates cariogenicity not by killing the organism but by coordinately disabling the molecular machinery of biofilm formation, acid production and oxidative-stress defense.

Bacteriostatic, anti-virulence profile

The MIC of 1250 µg/mL combined with the absence of any bactericidal endpoint (MBC > 2500 µg/mL; MBC/MIC > 2) firmly places SFN in the bacteriostatic category. This agrees with the report on the reference strain UA159, in which SFN likewise failed to produce a bactericidal effect yet markedly weakened cariogenic virulence [24]. The higher MIC observed here relative to laboratory strains is expected: clinical isolates frequently exhibit greater phenotypic robustness, thicker matrices and biofilm

Vol 14, No 2 (2026) DOI 10.5195/d3000/2026.1492

heterogeneity, and the present collection was dominated by strong biofilm producers. A bacteriostatic, anti-virulence action is increasingly viewed as advantageous, since it disarms the pathogen while exerting minimal selective pressure for resistance and sparing the protective commensal flora [13-15].

Suppression of *gtfC* and the structural collapse of biofilm

Among the three genes, *gtfC* was the most strongly repressed (≈99.5%). Glucosyltransferase C synthesizes the water-insoluble glucans that constitute the adhesive backbone of cariogenic biofilm, mediating both initial attachment and three-dimensional matrix architecture [5,6,10]. Near-complete suppression of *gtfC* provides a direct mechanistic explanation for the dose-dependent anti-biofilm effect documented in Figure 4: by collapsing glucan synthesis, SFN deprives the biofilm of its scaffold, impairing adhesion, cohesion and aggregation. This is fully consistent with the established principle that targeting *gtf* genes selectively undermines *S. mutans* virulence without eradicating the species or perturbing commensal streptococci [28,29], and mirrors the action of other natural products such as tea catechins and shikimic acid [29,30].

Suppression of ldh and the chemistry of demineralization

Down-regulation of *ldh* (≈97%) targets acidogenicity, the proximate cause of enamel dissolution. Lactate dehydrogenase is the principal enzyme converting glycolytic pyruvate to lactic acid, and its activity governs the magnitude of the plaque pH drop that initiates demineralization [8,29]. A reduced *ldh* transcript pool implies a diminished capacity to acidify the tooth surface, meaning that SFN attacks not only the structural basis of caries (the biofilm) but also its chemical driver (acid production). This dual action distinguishes anti-virulence agents that merely loosen the biofilm from those, like SFN, that also blunt the cariogenic insult itself.

Suppression of sodA: a novel oxidative-stress dimension

The strong repression of *sodA* (≈97%) is, to our knowledge, a novel observation for SFN against *S. mutans*. Superoxide dismutase neutralizes superoxide radicals and is central to the aerotolerance and stress survival that allow this organism to persist within the fluctuating redox environment of dental plaque [9,12]. As an isothiocyanate bearing a reactive –N=C=S group, SFN readily conjugates protein thiols and perturbs cellular redox homeostasis [16,18,31]. By suppressing *sodA*, SFN is expected to strip the organism of a first-line antioxidant defense, rendering it more vulnerable to oxidative stress within the biofilm and less able to maintain a stable cariogenic community. This oxidative-stress axis was not addressed in earlier work on SFN and *S. mutans* [24], and it adds a mechanistically distinct dimension to the compound's anti-virulence profile.

Evidence for a coordinated multi-target mechanism

The correlation and PCA analyses reinforce a multi-target interpretation. The strong co-regulation of *gtfC* and *sodA*, together with clean PCA separation of treated and untreated profiles along a dominant first component, indicates that SFN imposes an integrated transcriptional shift across adhesion, acidogenesis and oxidative defense simultaneously, rather than acting on a single pathway. Such behavior is consistent with the recognized multi-target pharmacology of isothiocyanates [18,21,31]. It is plausible that these effects are partly mediated through upstream regulatory systems known to control these genes, notably the *VicRK* two-component system, the over-expression of which up-regulates the *gtf* genes [32,33]; this hypothesis warrants direct investigation.

Clinical relevance and limitations

From a translational standpoint, an agent that suppresses biofilm, acid production and stress defense at sub-inhibitory, non-lethal concentrations, while displaying the well-documented safety of SFN [19,20], is an attractive candidate for caries-preventive formulations. Several limitations temper these conclusions. The work relies on single-species in-vitro assays that do not reproduce the ecological complexity of multispecies oral biofilms or the salivary and host environment. Transcriptional analysis was restricted to three representative genes; broader transcriptomic profiling, together with enzyme-activity and protein-level assays, would more fully delineate the regulatory network, including the *VicRK* and *ComDE* systems [32,34]. The fold-change data also exhibited considerable inter-isolate variability, reflecting the genuine biological heterogeneity of clinical isolates. Finally, in-vivo validation and formal biocompatibility testing are required before clinical application.

Conclusion

Sulforaphane acts as a bacteriostatic, multi-target anti-virulence agent against clinical *S. mutans* isolates. Without killing the cell, it simultaneously dismantles the three core determinants of cariogenicity — biofilm/EPS synthesis (*gtfC*), acid production (*ldh*) and oxidative-stress defense (*sodA*) — by more than 97% at sub-inhibitory concentrations, with a clear dose-dependent anti-biofilm effect and a coordinated, multi-gene transcriptional signature. These findings position SFN as a promising natural candidate for caries control with low resistance-selection potential and justify further multispecies, mechanistic and in-vivo investigation.

Declarations

Ethics approval: Approved by the Medical Ethics Committee, Middle Technical University, Baghdad, Iraq (No. MEC: 121; 07/05/2025).
Funding: None declared.
Conflict of interest: The author declares no conflict of interest.
Data availability: Data are available from the corresponding author on reasonable request.

References

1. Lemos JA, Palmer SR, Zeng L, Wen ZT, Kajfasz JK, Freires IA, et al. The biology of Streptococcus mutans. Microbiol Spectr. 2019;7(1):GPP3-0051-2018.
2. Machiulskiene V, Campus G, Carvalho JC, Dige I, Ekstrand KR, Jablonski-Momeni A, et al. Terminology of dental caries and dental caries management: consensus report of a workshop organized by ORCA and Cariology Research Group of IADR. Caries Res. 2020;54(1):7-14.
3. Bowen WH, Burne RA, Wu H, Koo H. Oral biofilms: dynamic ecosystems shaping integration of microbial communities and host physiology. Trends Microbiol. 2018;26(3):229-42.
4. Lemos JA, Quivey RG, Koo H, Abranches J. Streptococcus mutans: a new Gram-positive paradigm? Microbiology (Reading). 2013;159(Pt 3):436-45.
5. Bowen WH, Koo H. Biology of Streptococcus mutans-derived glucosyltransferases: role in extracellular matrix formation of cariogenic biofilms. Caries Res. 2011;45(1):69-86.
6. Koo H, Falsetta ML, Klein MI. The exopolysaccharide matrix: a virulence determinant of cariogenic biofilm. J Dent Res. 2013;92(12):1065-73.
7. Matsui R, Cvitkovitch D. Acid tolerance mechanisms utilized by Streptococcus mutans. Future Microbiol. 2010;5(3):403-17.
8. Lemos JA, Abranches J, Burne RA. Responses of cariogenic streptococci to environmental stresses. Curr Issues Mol Biol. 2005;7(1):95-107.
9. Higuchi M, Yamamoto Y, Poole LB, Shimada M, Sato Y, Takahashi N, et al. Functions of two types of NADH oxidases in energy metabolism and oxidative stress of Streptococcus mutans. J Bacteriol. 1999;181(19):5940-7.
10. Zheng T, Jing M, Gong T, Yan J, Wang X, Xu M, et al. Regulatory mechanisms of exopolysaccharide synthesis and biofilm formation in Streptococcus mutans. J Oral Microbiol. 2023;15(1):2225257.
11. Quivey RG, Kuhnert WL, Hahn K. Adaptation of oral streptococci to low pH. Adv Microb Physiol. 2000;42:239-74.
12. Nakayama K. Rapid viability loss on exposure to air in a superoxide dismutase-deficient

Vol 14, No 2 (2026) DOI 10.5195/d3000/2026.1492

mutant of Porphyromonas gingivalis. J Bacteriol. 1994;176(7):1939-43.
13. de la Fuente-Nunez C, Cesaro A, Hancock REW. Antibiotic failure: beyond antimicrobial resistance. Drug Resist Updat. 2023;71:101012.
14. Cao X, Cheng XW, Liu YY, Dai HW, Gan RY. Inhibition of pathogenic microbes in oral infectious diseases by natural products: sources, mechanisms, and challenges. Microbiol Res. 2023;279:127548.
15. Fux CA, Costerton JW, Stewart PS, Stoodley P. Survival strategies of infectious biofilms. Trends Microbiol. 2005;13(1):34-40.
16. Vanduchova A, Anzenbacher P, Anzenbacherova E. Isothiocyanate from broccoli, sulforaphane, and its properties. J Med Food. 2019;22(2):121-6.
17. Fahey JW, Zalcmann AT, Talalay P. The chemical diversity and distribution of glucosinolates and isothiocyanates among plants. Phytochemistry. 2001;56(1):5-51.
18. Romeo L, Iori R, Rollin P, Bramanti P, Mazzon E. Isothiocyanates: an overview of their antimicrobial activity against human infections. Molecules. 2018;23(3):624.
19. Calabrese EJ, Kozumbo WJ. The phytoprotective agent sulforaphane prevents inflammatory degenerative diseases and age-related pathologies via Nrf2-mediated hormesis. Pharmacol Res. 2021;163:105283.
20. Houghton CA. Sulforaphane: its 'coming of age' as a clinically relevant nutraceutical in the prevention and treatment of chronic disease. Oxid Med Cell Longev. 2019;2019:2716870.
21. Davidian, O.M., Tuturov, N.S., Lukyanova, E.A., Kitaeva, A.B., Konstantinova, E.E., Marchenko, D.M. and Baranova, A.A., 2026. Gender differences in dental caries intensity in young and preschool children living in Moscow.
22. Nowicki D, Krause K, Szamborska P, Zawadzka A, Herman-Antosiewicz A, Wegrzyn G, et al. Induction of the Escherichia coli stringent response is a strategy used by sulforaphane to eliminate enterohemorrhagic E. coli. Front Microbiol. 2020;11:1610.
23. Deramaudt TB, Ali M, Vinit S, Bonay M. Sulforaphane reduces intracellular survival of Staphylococcus aureus in macrophages through inhibition of JNK and p38 MAPK-induced inflammation. Int J Mol Med. 2020;45(6):1927-41.
24. Yu M, Chen Y, Dong S, Chen Z, Jiang X, Wang Y, et al. Sulforaphane as a promising anti-caries agent: inhibitory effects on Streptococcus mutans and caries control in a rat model. Front Microbiol. 2025;15:1427803.
25. de Souza MQ, Bierhals DV, Reis AJ, Chimara E, Vianna JS, von Groll A, et al. 2,3,5-Triphenyltetrazolium chloride as colorimetric indicator for drug susceptibility testing against nontuberculous mycobacteria. Diagn Microbiol Infect Dis. 2024;108(1):116096.
26. Hasan ME, Shahriar A, Shams F, Nath AK, Emran TB. Correlation between biofilm formation and antimicrobial susceptibility pattern toward extended spectrum beta-lactamase producing uropathogenic bacteria. J Basic Clin Physiol Pharmacol. 2020;32(1):12-21.
27. Livak KJ, Schmittgen TD. Analysis of relative gene expression data using real-time quantitative PCR and the 2^-DDCt method. Methods. 2001;25(4):402-8.
28. Zhang Q, Ma Q, Wang Y, Wu H, Zou J. Molecular mechanisms of inhibiting glucosyltransferases for biofilm formation in Streptococcus mutans. Int J Oral Sci. 2021;13(1):30.
29. Xu X, Zhou XD, Wu CD. The tea catechin epigallocatechin gallate suppresses cariogenic virulence factors of Streptococcus mutans. Antimicrob Agents Chemother. 2011;55(3):1229-36.
30. Zhang Z, Yang Y, Sun Q, Zeng W, Li Y. Inhibition of biofilm formation and virulence factors of cariogenic oral pathogen Streptococcus mutans by shikimic acid. Microbiol Spectr. 2022;10(4):e0119922.
31. Subramaniam M, et al. Anti-inflammatory therapeutic mechanisms of isothiocyanates: insights from sulforaphane. Biomedicines. 2024;12(6):1169.
32. Senadheera MD, Guggenheim B, Spatafora GA, Huang YC, Choi J, Hung DC, et al. A VicRK signal transduction system in Streptococcus mutans affects gtfBCD, gbpB, and ftf expression, biofilm formation, and genetic competence development. J Bacteriol. 2005;187(12):4064-76.
33. Smith EG, Spatafora GA. Gene regulation in S. mutans: complex control in a complex environment. J Dent Res. 2012;91(2):133-41.
34. Kaur G, Rajesh S, Princy SA. Plausible drug targets in the Streptococcus mutans quorum sensing pathways to combat dental biofilms and associated risks. Indian J Microbiol. 2015;55(4):349-56.

Table 1. Primer sequences used for quantitative RT-PCR.

Gene	Primer sequence (5′→3′)	Tm (°C)	Amplicon (bp)
sodA	F: TCGCAAACGCTAATGCGGC R: AATTGCTGCGGCTACTTCCG	61–62	203
ldh	F: ACTCGCCTCGATCTCGTTGG R: GGACTGAACGCGCATCAACA	62	244
gtfC	F: AGCAACGGATACAGGGGACC R: GTGTAGCGCACCAAACCAGC	62	216
16S rRNA	F: TCGGAGTCAACGGATTTGGTC R: AGCATCGCCCCACTTGATTT	62	305

Table 2. Mean inhibition-zone diameters of SFN against S. mutans isolates (n = 25).

SFN concentration	Inhibition zone (mm, mean ± SD)
5% (50 mg/mL)	17.8 ± 0.55
2.5% (25 mg/mL)	14.8 ± 0.58
1.25% (12.5 mg/mL)	13.7 ± 0.74
0.62% (6.2 mg/mL)	10.9 ± 1.54

Vol 14, No 2 (2026) DOI 10.5195/d3000/2026.1492

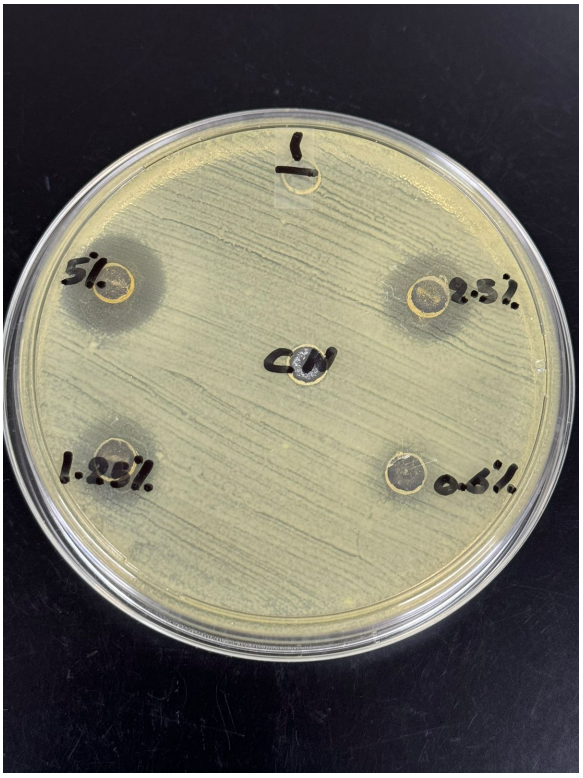

Figure 1A. Agar-well diffusion plate showing inhibition zones produced by SFN at 5%, 2.5%, 1.25% and 0.62% against a representative S. mutans isolate; CN denotes the solvent control.

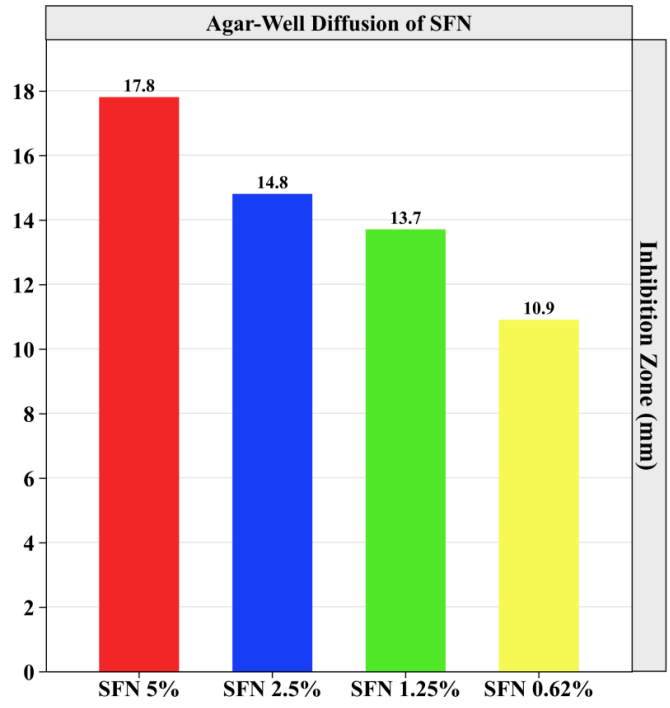

Figure 1B. Mean inhibition-zone diameters (mm) of SFN across the four tested concentrations (n = 25).

Vol 14, No 2 (2026) DOI 10.5195/d3000/2026.1492

Table 3. Mean percentage inhibition and growth outcome of S. mutans across SFN concentrations (n = 25).

SFN (µg/mL)	Mean inhibition (%)	Growth (TTC)
2500	91.8 ± 0.01	No growth (–)
1250 (MIC)	90.2 ± 0.01	No growth (–)
625	44.0 ± 0.14	Growth (+)
313	33.5 ± 0.54	Growth (+)
156	16.7 ± 0.09	Growth (+)
78	12.0 ± 0.08	Growth (+)
39	5.8 ± 0.05	Growth (+)
19.5	2.3 ± 0.03	Growth (+)

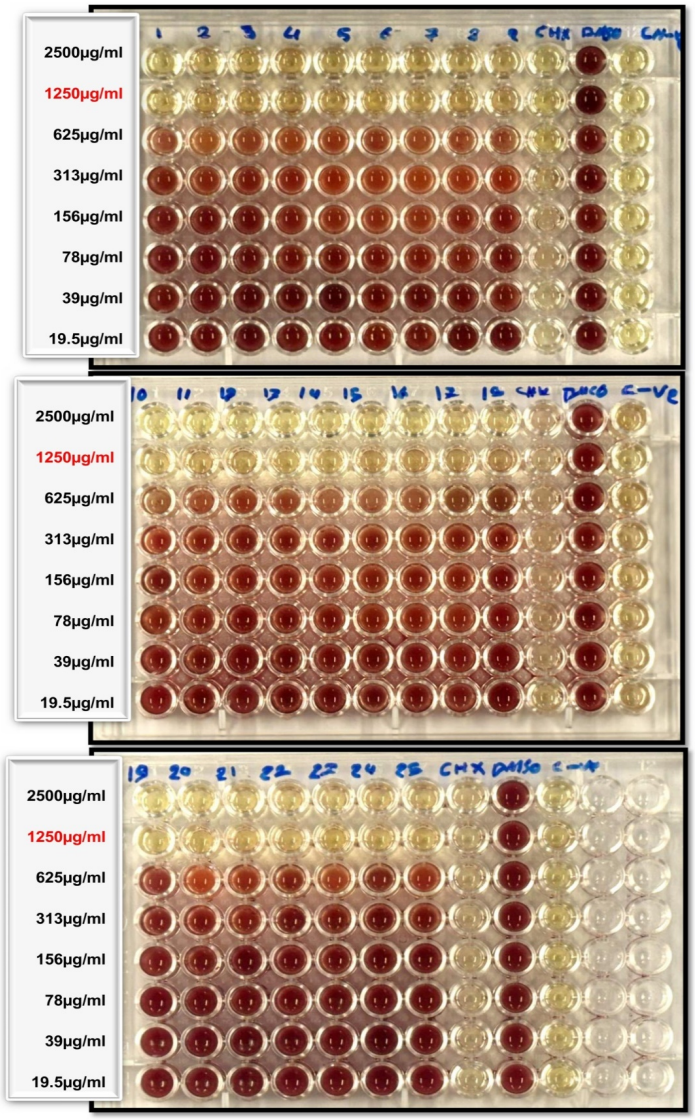

Figure 2A. Broth-microdilution MIC assay with TTC viability staining for the 25 isolates. Colorless wells indicate growth inhibition; red/pink wells indicate viable growth. Wells at 2500 and 1250 µg/mL remained colorless across all isolates, defining the MIC at 1250 µg/mL (highlighted).

Vol 14, No 2 (2026) DOI 10.5195/d3000/2026.1492

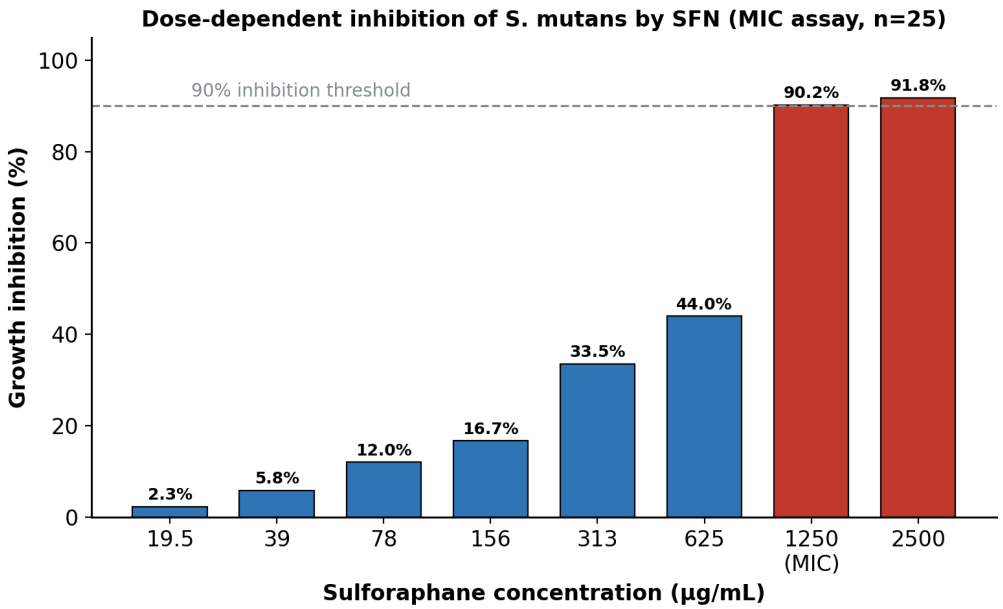

Figure 2B. Dose-dependent mean growth inhibition (%) of S. mutans by SFN; the dashed line marks the 90% inhibition threshold (mean, n = 25).

Table 4. Distribution of biofilm-forming capacity among the 25 clinical isolates.

Biofilm category	No. of isolates	Percentage
Strong	18	72%
Moderate	3	12%
Weak	4	16%
Total	25	100%

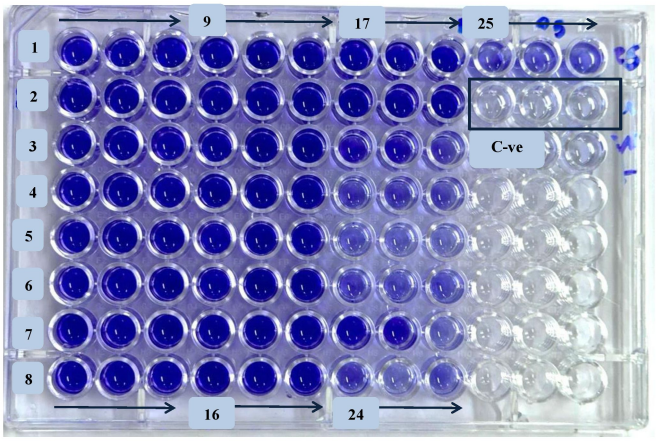

Figure 3A. Crystal-violet microtiter assay of biofilm formation by the 25 clinical isolates; intensity of staining reflects biofilm biomass. C-ve denotes the negative (sterility) control.

Vol 14, No 2 (2026) DOI 10.5195/d3000/2026.1492

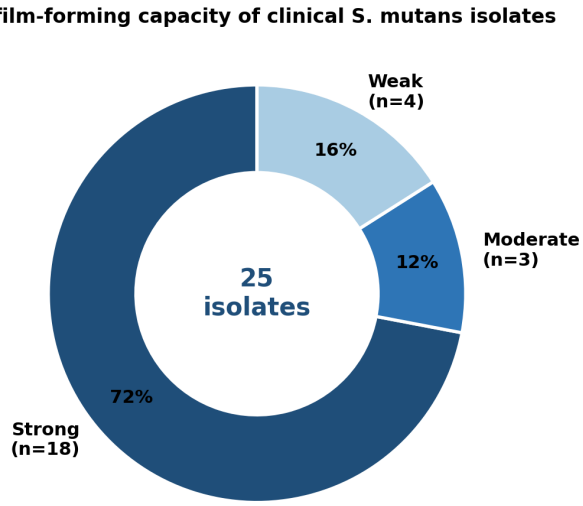

Figure 3B. Distribution of biofilm-forming capacity (strong/moderate/weak) among the 25 isolates.

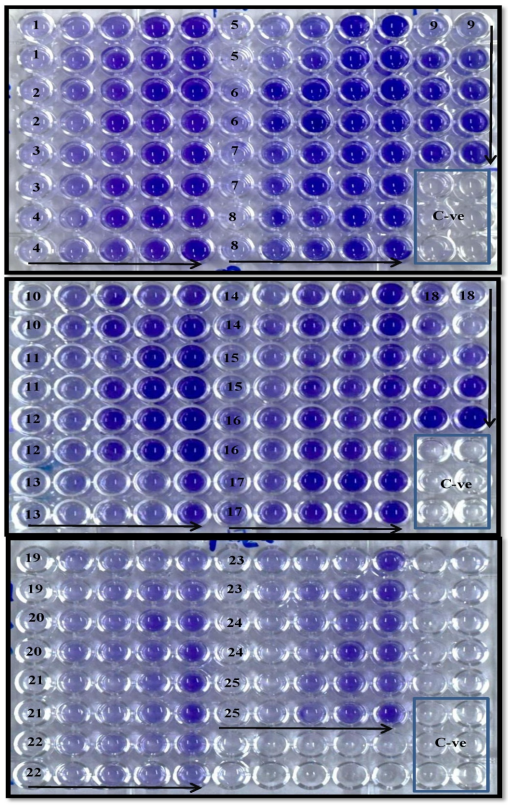

Figure 4A. Crystal-violet anti-biofilm assay: residual biofilm of the 25 isolates after treatment with serial SFN concentrations (1250–78 µg/mL, in duplicate); C-ve denotes the negative control.

Vol 14, No 2 (2026) DOI 10.5195/d3000/2026.1492

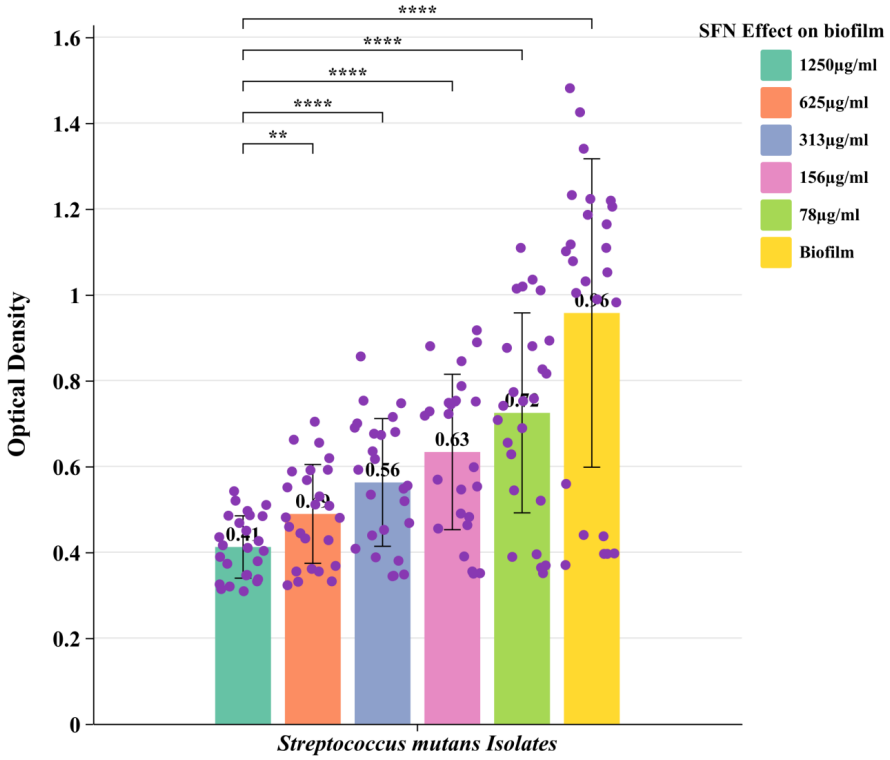

Figure 4B. Mean biofilm optical density of S. mutans across SFN concentrations versus the untreated biofilm control. ** $p < 0.01$; **** $p < 0.0001$ (mean ± SD, n = 25).

Figure 4C. Heatmap of mean biofilm optical density for each isolate (S1–S25) across SFN concentrations and the untreated biofilm control, showing dose-dependent biofilm reduction.

Vol 14, No 2 (2026) DOI 10.5195/d3000/2026.1492

Table 5. Relative expression (fold change, 2^-ΔΔCt) of target genes before and after SFN treatment (n = 25).

Gene	Control (mean ± SD)	SFN (mean ± SD)	Reduction	p-value
gtfC	2.571 ± 4.468	0.013 ± 0.020	↓99.5%	1.2×10^{-6}
sodA	1.732 ± 2.290	0.049 ± 0.065	↓97.2%	3.6×10^{-4}
ldh	2.787 ± 4.326	0.082 ± 0.157	↓97.0%	7.4×10^{-3}

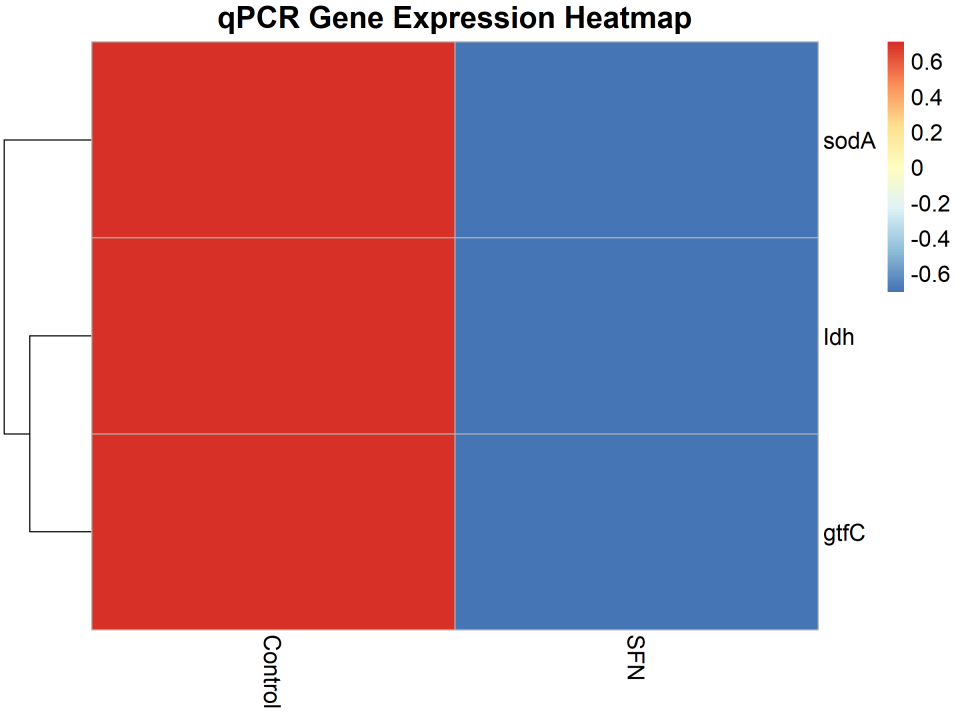

Figure 5. Expression heatmap of gtfC, sodA and ldh in control versus SFN-treated S. mutans, showing uniform down-regulation after treatment.

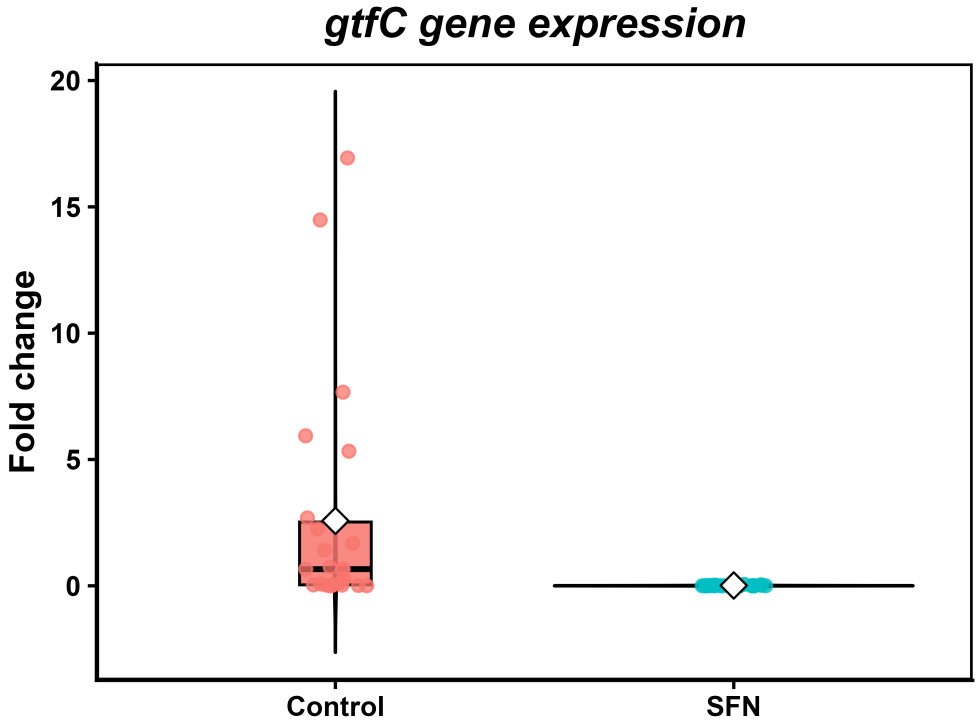

Figure 6A. Distribution of gtfC fold-change values in control and SFN groups (raincloud/violin plot).

Vol 14, No 2 (2026) DOI 10.5195/d3000/2026.1492

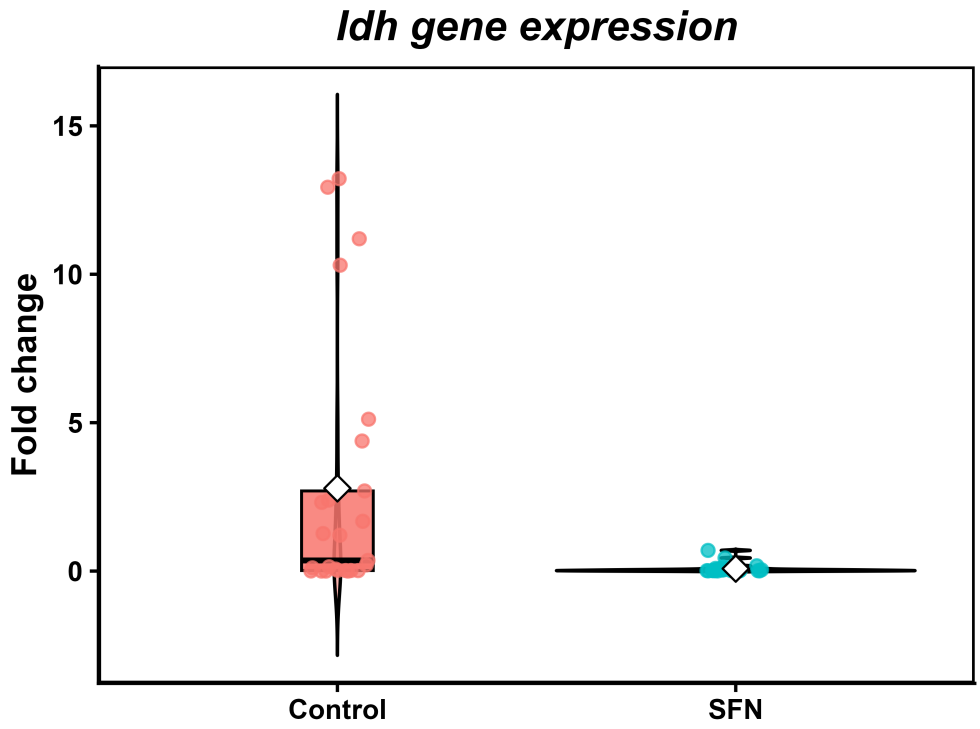

Figure 6B. Distribution of ldh fold-change values.

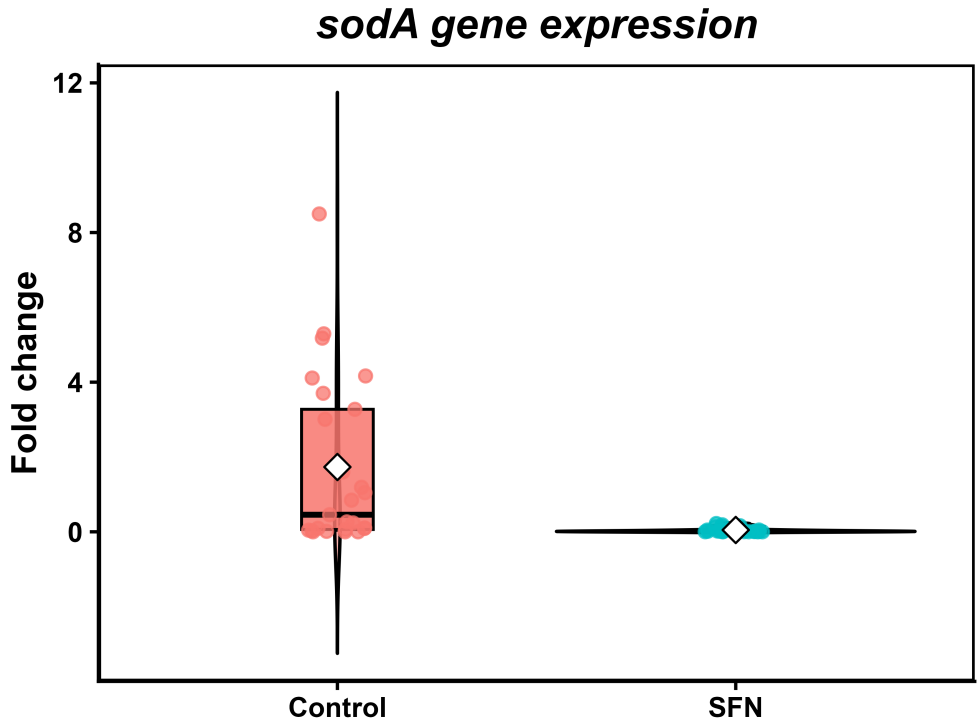

Figure 6C. Distribution of sodA fold-change values.

Vol 14, No 2 (2026) DOI 10.5195/d3000/2026.1492

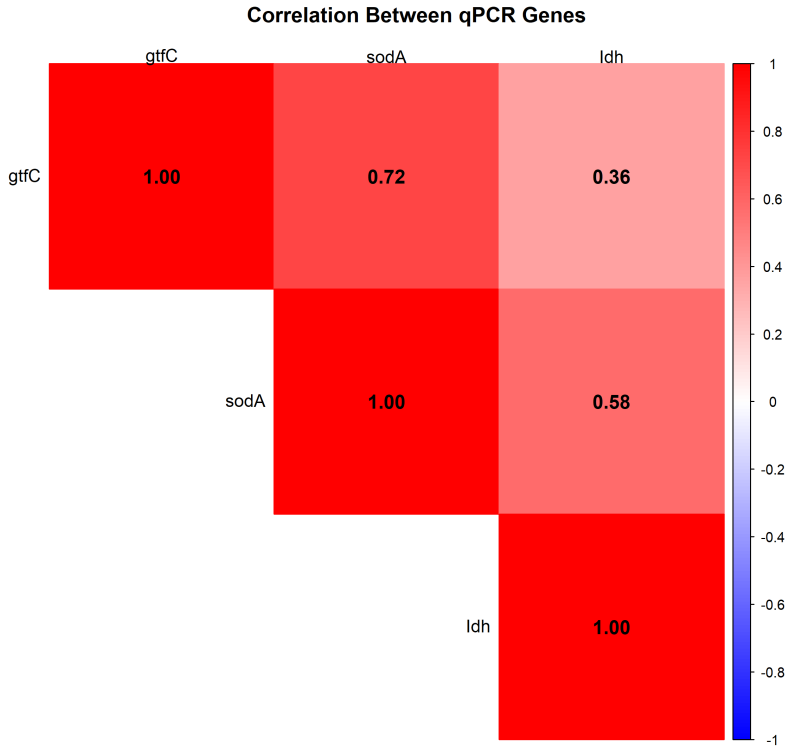

Figure 7. Pearson correlation matrix among gtfC, sodA and ldh fold-change values.

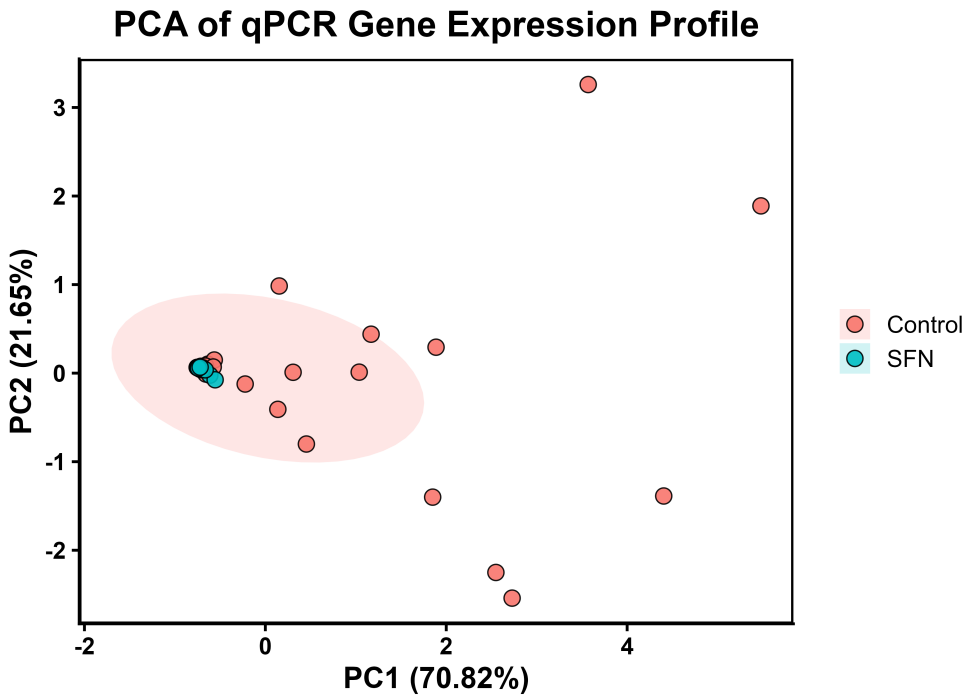

Figure 8. Principal component analysis of the three-gene expression profile, separating control from SFN-treated isolates (PC1 = 70.8%, PC2 = 21.7%).